Hindawi
International Journal of RF and Microwave Computer-Aided Engineering
Volume 2023, Article ID 2913342, 9 pages
https://doi.org/10.1155/2023/2913342

Research Article

The Design of Miniature Frequency Reconfigurable Antenna Based on Inductive Loading Technology

Yuqiu Shang,[1] **Qingsheng Zeng**,[2] **Qian Wang**,[1] **Xinwei Wang**,[1] **Gengqi Zheng**,[1] **and Feng Shang**[1]

[1]*School of Electronics Eng., Xi'an University of Post & Telecommunications, Xi'an, China*
[2]*School of Astronautics, Nanjing University of Aeronautics & Astronautics, Nanjing, China*

Correspondence should be addressed to Yuqiu Shang; shangyuqiu@nuaa.edu.cn

Received 11 April 2023; Revised 25 June 2023; Accepted 7 November 2023; Published 23 November 2023

Academic Editor: Chow-Yen-Desmond Sim

A circularly polarized (CP) and frequency reconfigurable microstrip antenna with loading inductive is presented in this paper. The designed antenna is comprised of a radiating patch, four short-circuited grounded metal posts, and four coupling branches. Each coupling branch has an end that is coupled to the shorted ground post and is also connected to the parasitic branches by means of a group of PIN diodes. By controlling the state of the PIN diodes connected to each parasitic branch, the working resonant frequency of the antenna can be changed. In order to further understand the mechanisms of operation of the antenna, the equivalent circuit model was built, and the circuit model of the antenna was analyzed, and this analysis was used for the development of the frequency reconfigurable microstrip patch antenna. Furthermore, the parameters of specific equivalent circuits can be solved by the three lengths of branch. Meanwhile, the calculated results derived from the given resonant frequency formula for the antenna are in good agreement with the simulation results of the antenna. Simulated results for the input impedance of the antenna are also in good agreement with the calculated values for the equivalent circuit. Finally, the antenna is fabricated and measured, and the measured results show that the antenna can not only achieve frequency reconfiguration at 1.14 GHz, 1.21 GHz, and 1.39 GHz but also accord well with the simulation value, while maintaining a compact size.

1. Introduction

With the rapid development of wireless communication technologies and applications in recent years, and to satisfy the requirements of many applications, such as mobile and satellite communications, base stations, cognitive radios, navigation, and remote sensing, the reconfigurable antennas and relevant techniques are researched for low cost and space-saving [1–5]. Especially, the frequency reconfigurable technology will meet the antenna operating in numbers of multisystems [5–8], which becomes an alternate antenna in a wide band wireless system.

The inherent disadvantage of microstrip antennas is their narrow bandwidth, which makes it difficult to realize multiband or broadband systems [9]. However, the frequency reconfigurable microstrip antenna is a suitable option for antennas working in a wide range of multiband and other special applications, owing to its limited size and low cost [10].

The transmission line model of microstrip patch antenna is proposed by Munson [10]. It is a common method for the analysis and optimization of microstrip patch antennas. Sun et al. have given the equivalent circuit of a microstrip antenna with a shorting probe [9, 11, 12]. The analysis method is using simulation software to calculate input impedance and resonance frequency of equivalent circuit and antenna. Further research and further documents always use this analysis method.

Many studies have reported the use of software simulation to analyze parasitic inductance or capacitance in antenna models in order to construct equivalent circuits. Similarly, in [9], the distributed parameters are utilized to

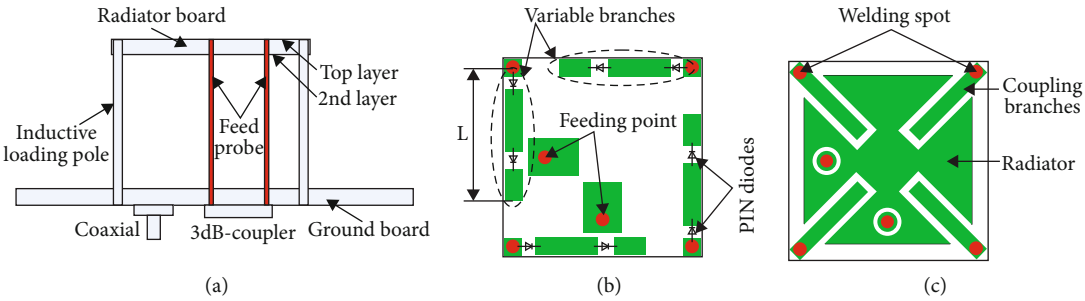

Figure 1: Illustration of the antenna. (a) Side view, (b) top layer, and (c) 2nd layer of the antenna.

increase the compactness of the antenna. Coupled between the patch and the branch is capacitance, and the larger the coupling size, the larger the coupling capacitance. In [13], an antenna is designed that has a frequency reconfigurable feature loaded by patch-shorted circuits and which can switch between three band operating frequencies of BeiDou navigation. As described in [14], two switches were inserted into the slot to serve as three reconfigurable frequency bands to achieve the triple-frequency switched antenna. A reconfigurable PIN diode is introduced in [15] in order to adjust the radiation path of current, which enables frequency reconfiguration. These frequency reconfigurable ways either change the current path of the antenna radiator or control the feed structure or feed mode, thus increasing the complexity and difficulty of the reconfiguration and reducing the radiation efficiency of the antenna. Whereas in our previous work [16], a novel method was proposed by changing the equivalent capacitance of the patch itself by changing the length of the variable branch, thereby obtaining the frequency reconstruction. Unfortunately, this work only gives the preliminary simulation results and does not involve the specific parameter values of the equivalent circuit of the antenna, the in-depth discussion of the equivalent circuit, and the verification of the fabricated antenna.

The analysis shows that changing the length of the variable branch will change its corresponding equivalent capacitance, thus changing its resonant frequency. In this paper, three branch lengths corresponding to three capacitance values are used to determine or solve lumped parameters of equivalent circuits. The resonant frequency of the antenna is derived from the resonant frequency calculation formula of the circuit. Therefore, this research can not only determine the consistency of the input impedance of the antenna and the equivalent circuit but also determine the accuracy of the lumped parameters of each component in the circuit and further determine the accuracy of the resonant frequency. At present, there are few reports about this method.

A frequency reconfigurable antenna is presented in this paper, which is a further in-depth study of our previous work [16]. By using PIN diodes and four variable branches, the operation frequency could be controlled at about 1.14 GHz, 1.21 GHz, and 1.39 GHz. The $|S_{11}|$ is below -15.7 dB at all operation frequencies, and the measured gain is about 1 dB at 1.14 GHz, 1.6 dB at 1.21 GHz, and 2.39 dB at 1.39 GHz. The dimension is only $20 \times 20 \times 20\,\text{mm}^3$, while a bigger test board is used to fix the RF connector.

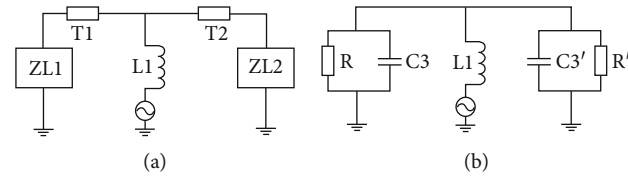

Figure 2: Transmission line model: (a) transmission line with loads and (b) input impedance of patch.

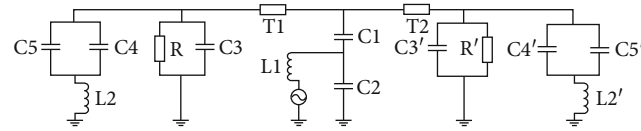

Figure 3: Equivalent circuit of the antenna.

2. Basic Mechanism of the Inductive Loading Frequency Reconfigurable Antenna

2.1. Basic Structure of Frequency Reconfigurable Antenna. The illustration of the proposed antenna is shown in Figure 1. At the top of the antenna, there is a radiator board, which is printed by radiator and branches on both sides. Four copper poles serving as inductors and supporting structures are connected between the radiator and the ground board. Meanwhile, two feeding probes could be used to support the radiator board either. The ground board is at the bottom of the antenna (see Figure 1(a)). The coaxial connector is fixed under the ground board, and a 3 dB 90° hybrid coupler is used to radiate CP wave from the antenna. Figures 1(b) and 1(c) are the two sides of the radiator board. The upper side is called as top layer, and the underside is called as 2nd layer. To facilitate control of the diodes inserted in the variable branches, variable branches are printed on the top layer. The radiator is designed as a rectangular microstrip patch and printed in the 2nd layer, with four slots etched at four corners. Each slot is arranged with a strip, which could bring the coupling capacitance and called as coupling branch (Figure 1(c)). Four coupling strips are connected to the inductance poles. The variable branches, which are connected to the inductance pole either, and L-shaped feeding patches are printed at the top layer. Each variable branch is consisted by three pieces of strips which are connected by 2 PIN diodes. And the states of

Table 1: Parameter of the equivalent circuit.

C1	C2	C3/C3'	C4/C4'	L1	L2/L2'	R/R'
1.67 pF	0.068 pF	22.95 pF	2.8 pF	3.82 nH	4.15 nH	170 Ω

PIN diodes could change the length of the variable branches. In this study, the length of variable branches is chosen as 1 mm, 9 mm, and 12 mm which corresponds to the resonant frequency of 1.39 GHz, 1.21 GHz, and 1.14 GHz separately.

The coupling branches and variable branches bring coupling capacitance between them and the radiating patch, while copper poles will generate parasitic inductance. Considering that the coupling capacitance is grounded by the parasitic inductance of the poles, this technique is known as inductive loading. When parasitic parameters change, the resonant frequency also changes, thus forming a frequency reconfigurable antenna.

2.2. Equivalent Circuit of Antenna. The popularity of the transmission line model may be gauged by the number of extensions to this model which have been developed in [17, 18]. The transmission line model of the rectangle microstrip antenna is shown in Figure 2. In this model, the rectangular microstrip antenna consists of a microstrip transmission line with a pair of loads at either end [19]. The input impedance or admittance is calculated by this model. The input impedance or admittance including the patch is considered the transmission line and the loads (Figure 2(a)). So, it must be an impedance generally. It should have a real part and an imaginary part (Figure 2(b)).

In Figure 2(b), the R, R', C3, and C3' only refer to the input impedance or the input admittance of the loads. The resistance R represents the radiation loss at both ends of the transmission line. C3 and C3' represent the whole reactance of the input impedance, which includes the distributed capacitance and inductance. The capacitance and inductance are related to the resonance frequency. In a circuit, see Figure 3, the resonant frequency could be calculated either if the C3 is a capacitance or the parallel capacitance and inductance, whose susceptance value is equal to $j\omega C3$.

The equivalent circuit of the proposed antenna is shown in Figure 3.

Because the CP is realized by the same but orthogonality linear polarization feed method, Figure 3 is an equivalent circuit of one of the linear polarizations. The phase difference between the two outputs of the 3 dB coupler is 90°, thus achieving CP. Where the L1, C1, and C2 are caused by the L-type feeding patch and the radiator and the ground, T1 and T2 are the length of the radiator patch which is divided by the feeding point, and R and R' are the radiation resistance of the antenna. C3 and C3' are the coupling capacitance between radiator and ground board. C4 and C4' are the coupling capacitance between radiator and coupling branches in the slot of the radiator. C5 and C5' are the coupling capacitance between radiator and variable branches. L2 and L2' are the inductive of the inductive loading pole [9]. Because C4 and C4' and C5 and C5' are connected to the ground through L2 and L2', the parallel relationship in Figure 3 is formed.

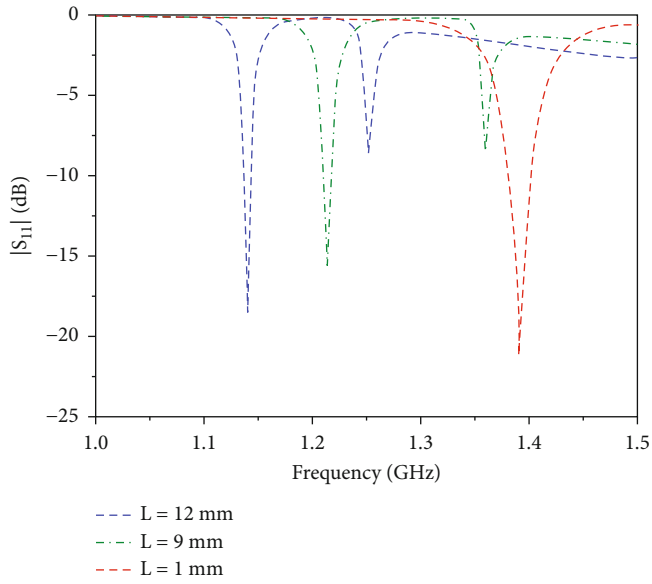

Figure 4: Simulation result of $|S_{11}|$.

2.3. Equivalent Circuit of Antenna. The resonant frequency of the antenna is determined by the above parameters, which is not mentioned in our literature [16]. C5 and C5' are controlled by the length of the variable branches. The states of the diodes are used to control the length of these branches. Therefore, the change of parameters leads to the reconstruction of antenna resonant frequency.

The two diodes of each branch exhibit transmission behavior when they are both on, and the resonant frequency decreases as the branch is extended. Nonetheless, when two diodes of each branch are turned off, the coupling capacitance between the branch and the radiator patch is eliminated. Therefore, C5 and C5' are nearer to zero.

So, the resonance frequency could be calculated by the half-side circuit of Figure 3. It is given in

$$\omega = \sqrt{\frac{C3 + C4 + C5}{L2 \times C3 \times (C4 + C5)}}. \quad (1)$$

Calculate the parameter values of the equivalent circuit in Figure 3 through simulation and solving Formula (1), as shown in Table 1.

C5 and C5' are the capacitance of variable branches. The length is corresponding to the coupling capacitance between branches and radiator. In this study, the branches are divided into three segments while connected by two PIN diodes. When the length is 12 mm, 9 mm, and 1 mm, the coupling capacitance is 3.05 pF, 2.26 pF, and 0.85 pF. Using Formula (1), the resonance frequencies of the antenna are 1.144 GHz, 1.214 GHz, and 1.393 GHz.

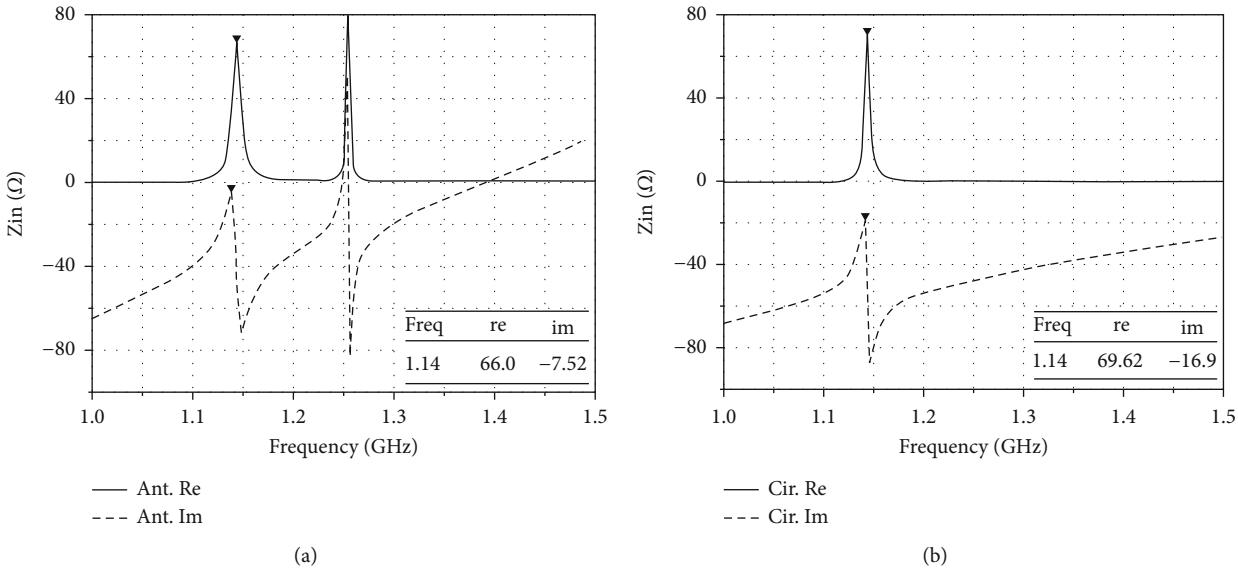

Figure 5: Input impedance comparison of antenna and circuit ($L = 12$ mm): (a) antenna simulation result and (b) equivalent circuit simulation result.

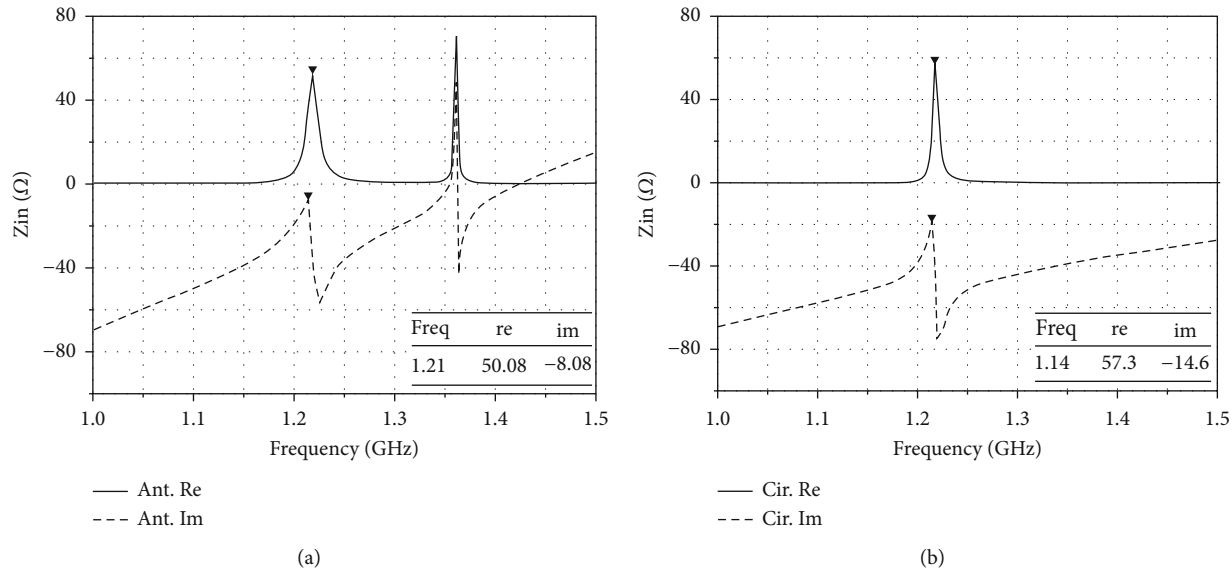

Figure 6: Input impedance comparison of antenna and circuit ($L = 9$ mm): (a) antenna simulation result and (b) equivalent circuit simulation result.

3. Simulation of the Antenna

3.1. Resonance Frequency of Antenna. As calculated previously by Formula (1), the resonance frequency is 1.144 GHz, 1.214 GHz, and 1.393 GHz. Using antenna simulation software, the resonance frequency could be gained either.

Figure 4 shows the simulation results of the antenna reflection coefficient in several different states, in which the lengths of the variable branches are 12 mm, 9 mm, and 1 mm, and the resonant frequencies of the corresponding antennas are 1.140 GHz, 1.216 GHz, and 1.392 GHz, respectively. The $|S_{11}|$ of three resonance frequencies is -18.7 dB, -15.7 dB, and -21.7 dB, respectively. The simulated results agree well with the calculated results.

3.2. Input Impedance Simulation of the Antenna and Equivalent Circuit. The input impedance of the antenna can be calculated by the antenna simulation software and the equivalent circuit model of the antenna. A simulation of the results is depicted in Figures 5–7. It is the impedance simulation results of three frequencies related to three lengths (L) of variable branches.

Figure 5(a) shows the input impedance curve with the branch length of 12 mm, while the C5 = C5$'$ = 3.05 pF. Compared with the simulation result of equivalent circuit in

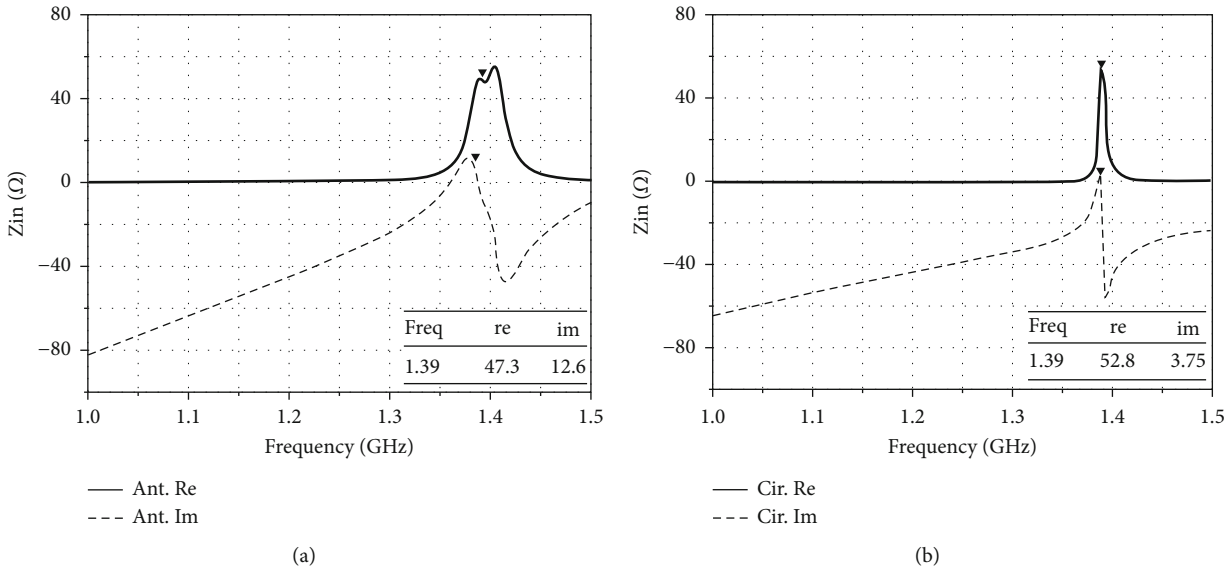

FIGURE 7: Input impedance comparison of antenna and circuit ($L = 1$ mm): (a) antenna simulation result and (b) equivalent circuit simulation result.

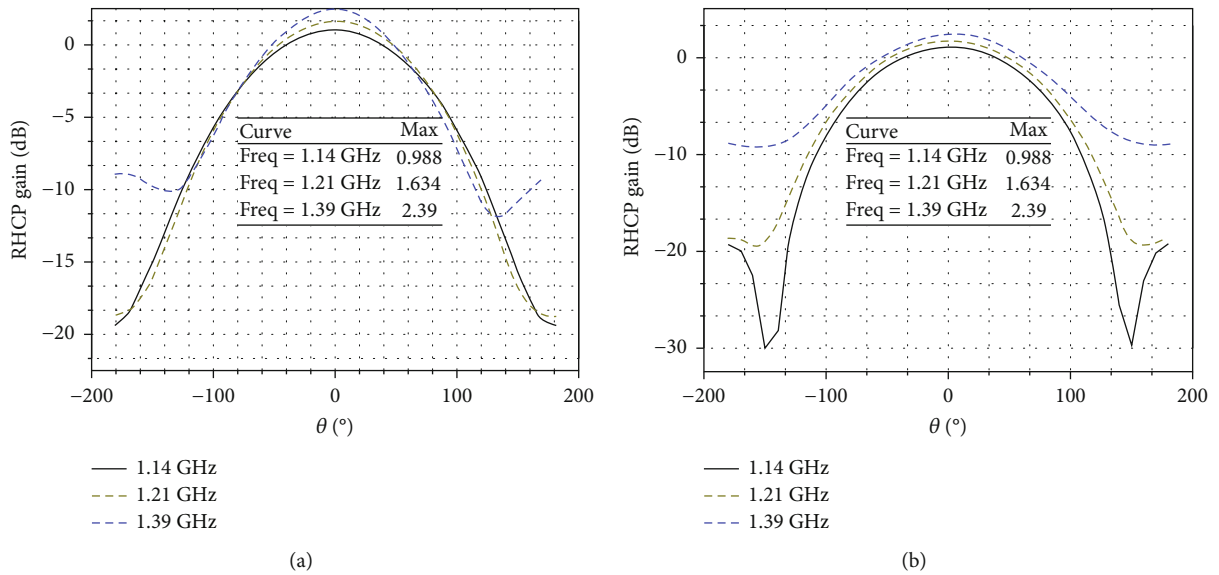

FIGURE 8: Radiation pattern: (a) E-plane pattern and (b) H-plane pattern.

Figure 5(b), the difference of the real part is only 3 Ω while the imaginary part is 7 Ω. Figure 6 is the input impedance curve with the branch length of 9 mm, while the $C5 = C5' = 2.26$ pF. Compared with the simulation result of the antenna, the difference of the real part is 7 Ω while the imaginary part is 6 Ω. Figure 7 is the input impedance curve with the branch length of 1 mm, while the $C5 = C5' = 0.85$ pF. Compared with the simulation result of the antenna, the difference of the real part is 5 Ω while the imaginary part is 9 Ω. The results show that the simulation of the antenna software is in good agreement with the calculation curve of the equivalent circuit.

In the previous research, the input impedance of the microstrip antenna was calculated by software simulation, and then, the equivalent circuit model was built with this as the target, and the simulation software was used to approach the target to obtain the parameter values. It is based on comparing the input impedance curves of the antenna and the equivalent circuit, and the results of the two are consistent because of the same input impedance. In this paper, according to the equivalent circuit model, the resonant frequency calculation formula of the circuit is given. With fixed parameters (L2, C3, and C4), one of the three reconfigurable resonant frequencies can be obtained by Formula (1), and the input impedance and resonant frequency of L2, C3, and C4 are adjusted to be consistent with the antenna simulation results. Then, Formula (1) is used to calculate C5 at the other two reconfigurable frequencies, and

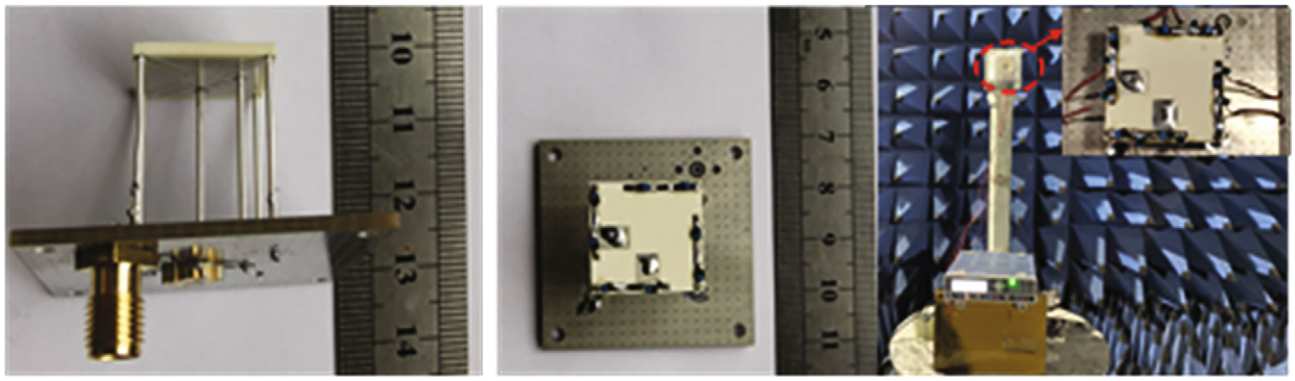

Figure 9: Fabricated photographs of the frequency reconfigurable antenna.

the correctness of L2, C3, and C4 is further verified when C5 is calculated.

3.3. Radiation Pattern of the Frequency Reconfigurable Antenna. An analysis of the performance of the proposed antenna at different reconstruction frequencies is presented. The frequency reconstruction can only be achieved by adjusting the state of the PIN diode embedded in each variable branch, as well as obtaining a compact structure for the antenna.

Figure 8 depicts the radiation pattern of the proposed antenna at three frequency points in two orthogonal planes. As a result, the simulated gains at the three reconstructed frequency points are 1 dB, 1.6 dB, and 2.4 dB, and the corresponding 3 dB beamwidths are also 135°, 125°, and 102°, showing a wide beam characteristic. Moreover, the PIN diode embedded for reconfiguration has a slight effect on the radiation pattern. The radiation characteristics of the wide beam indicate that the antenna has the potential to be applied in satellite navigation systems.

4. Measurement and Discussion

Figure 9 shows the fabricated and test scene of the antenna. The variable stripes with diodes are etched on the top layer, which is convenient for controlling the reconfiguration. The radiator has printed the 2nd layer, which did not influence the radiation.

The state of the diode used for reconstruction is controlled by the DC bias circuit. The schematic diagram of the control circuit is shown in Figure 10, two capacitors could prevent the DC shorted to each other, and the two inductors could prevent the RF current leak through the DC conductor line. The states of antenna change with the states of diodes are shown in Table 2.

The measured $|S_{11}|$ is shown in Figure 11. Compared with Figure 4, the resonant frequency of measurement is fit to the simulation results. The radiation pattern measured results are shown in Figure 12. Compared with simulation results, the pattern is matched to each other. The simulated and measured gains are slightly different. The simulation and measured gains are shown in Table 3.

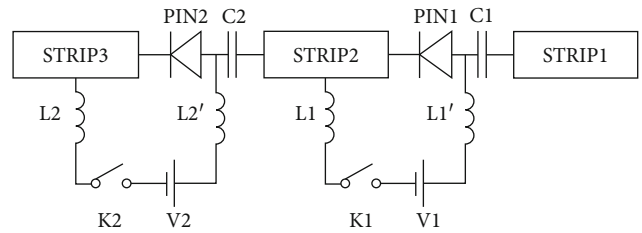

Figure 10: Schematic diagram of the control circuit.

Table 2: State control of the diodes.

Frequency (GHz)	1.39	1.21	1.14
PIN1	OFF	ON	ON
PIN2	OFF	OFF	ON

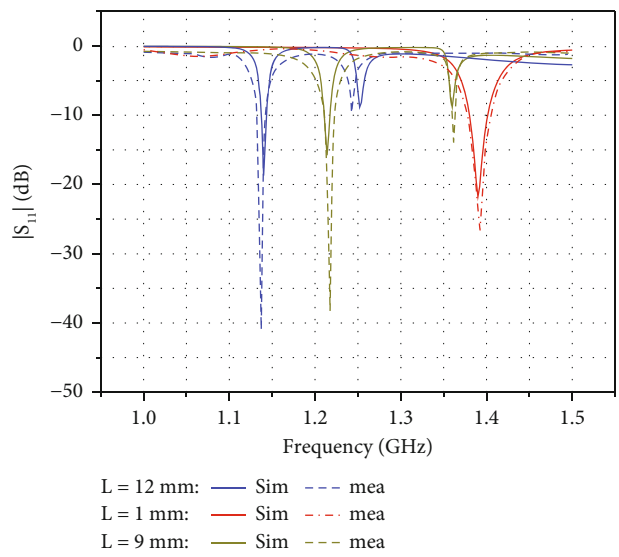

Figure 11: Measured and simulated results of $|S_{11}|$.

Measurement results are a bit lower. It is caused by the loss of the feeding line and the substrate material. In the simulation, the loss tangent is given. But it is not very accurate,

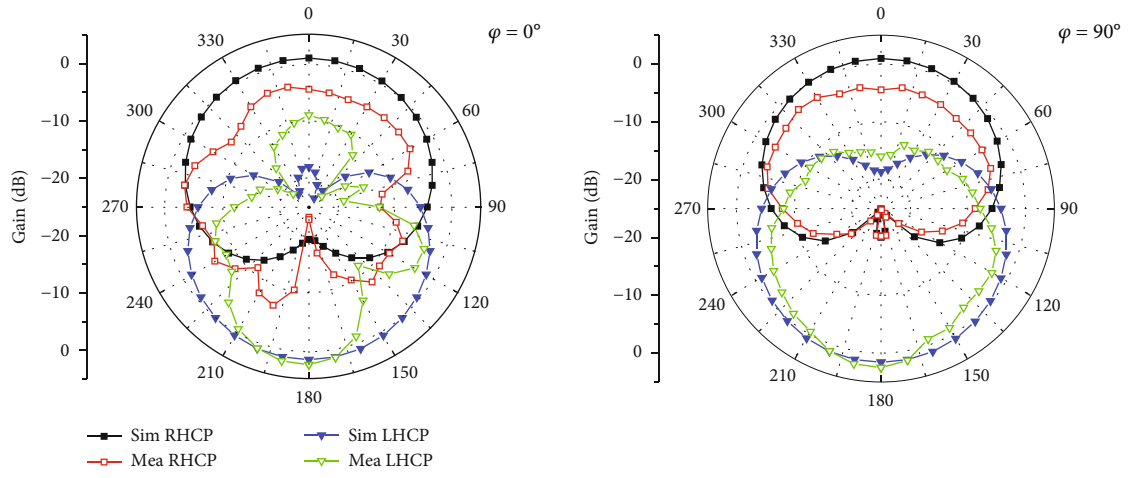

(a) 1.14 GHz

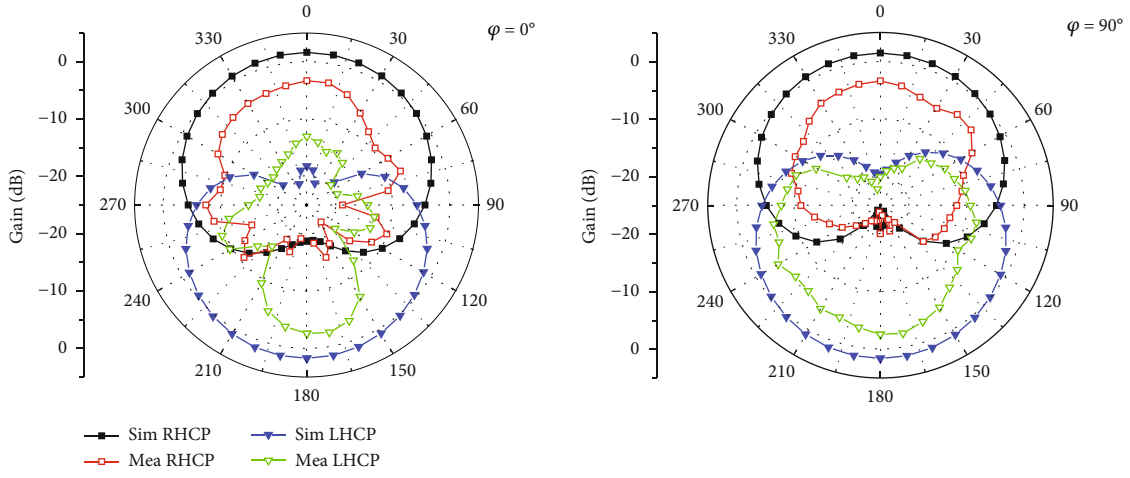

(b) 1.21 GHz

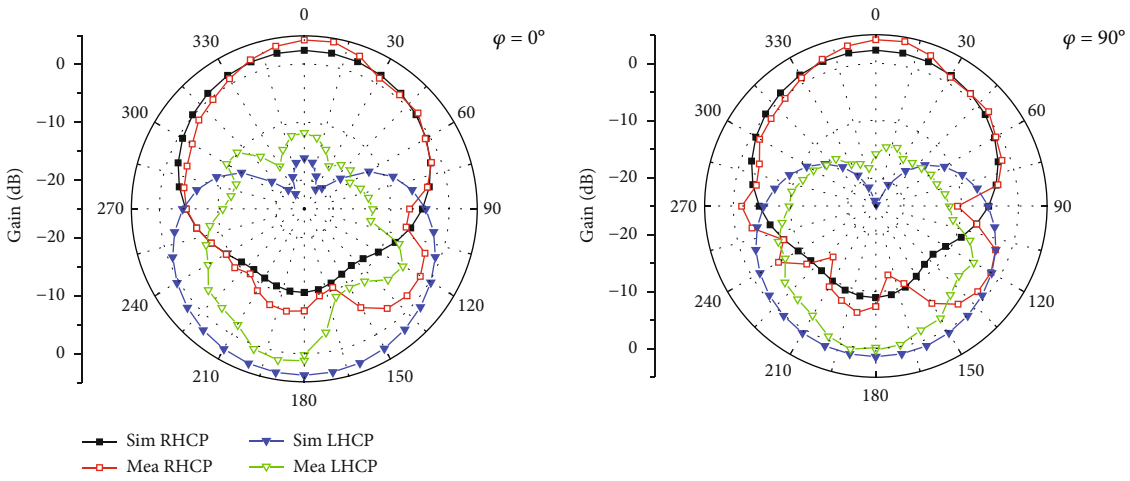

(c) 1.39 GHz

Figure 12: Measured and simulated results of the radiation pattern of the antenna.

as given by the manufacturer. And the measurement error has always existed. This can cause the difference between simulations and measurements. Measurement results are very near to the simulation results. Figure 12 shows the radiation patterns of three frequency points, respectively. It can be seen from the figure that the measured results show good circular polarization and wide beamwidth performances. The measured 3 dB beamwidths of the three frequency points are 140°, 111°, and 102°, respectively. At the same time, Figure 13 also shows the efficiency and axial ratio of

Table 3: Comparison of gain between simulation and measurement.

Frequency (GHz)	Simulated (dBi)		Measurement (dBi)	
	E-plane	H-plane	E-plane	H-plane
1.14	0.988	0.988	0.788	0.708
1.21	1.634	1.634	1.125	1.197
1.39	2.39	2.39	2.255	2.215

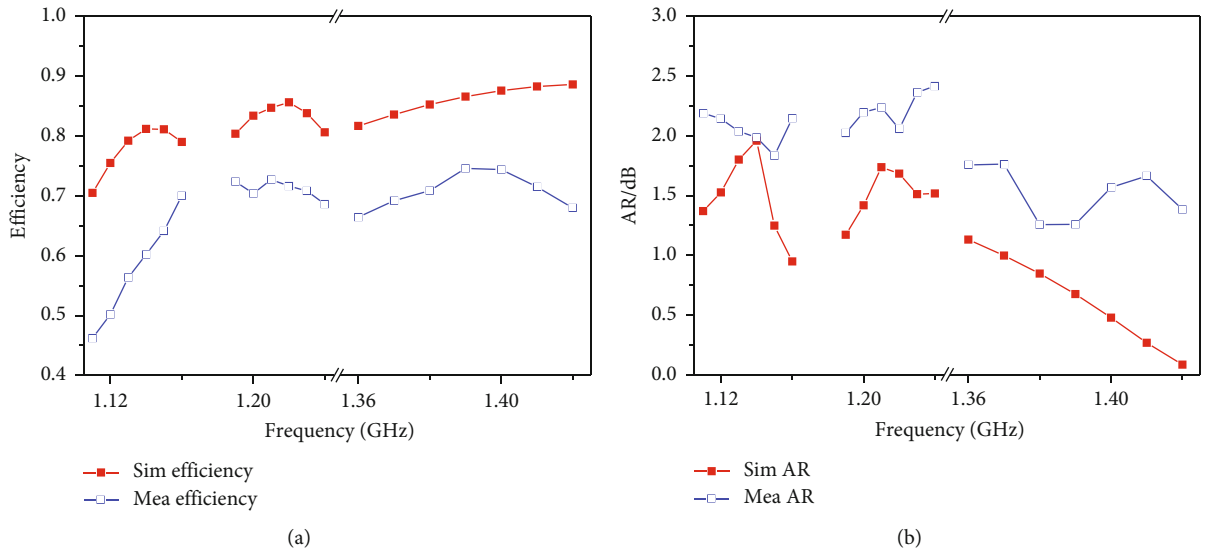

Figure 13: Measured and simulated results of efficiencies and axial ratio. (a) Efficiencies and (b) axial ratio.

the simulated and measured three frequency points, respectively. It can be seen from the figure that the efficiency of the antenna at these three reconfigurable frequency points is over 80%. According to the measured axial ratio, the designed reconfigurable antenna also shows good circular polarization characteristics.

5. Conclusions

This paper presents a frequency reconfigurable antenna and designs and analyzes the measurements of the antenna. By in-depth investigation, the equivalent circuit model of the frequency reconfigurable antenna is given, and the formula for calculating the resonant frequency of the antenna is derived according to the circuit model. Through the calculation of the formula, the results show that the calculation results are in good agreement with the simulation and measurement results. The realization of frequency reconfiguration is that the PIN diode is used to change the length of the variable branches which are printed on the top layer. The resonant frequency of the antenna is controlled by the state of diodes. Changing the length of the branch does not change the pattern. By adding more diodes, the proposed design can obtain more frequency substitution values. This method can be used for patch antennas operating in other frequency bands. The area of the radiator is smaller than the microstrip antenna without the loading probe.

Data Availability

All data are displayed and analyzed in the manuscript.

Conflicts of Interest

The authors declare that they have no conflicts of interest.

Acknowledgments

This study is sponsored by the Shaanxi Province Science and Technology Department (2021ZDLGY08-03) and the National Natural Science Foundation of China (41474027).

References

[1] C. J. Panagamuwa, A. Chauraya, and J. C. Vardaxoglou, "Frequency and beam reconfigurable antenna using photoconducting switches," *IEEE Transactions on Antennas and Propagation*, vol. 54, no. 2, pp. 449–454, 2006.

[2] Y. Qian and Q. Chu, "A polarization-reconfigurable water-loaded microstrip antenna," *IEEE Antennas and Wireless Propagation Letters*, vol. 16, pp. 2179–2182, 2017.

[3] M. S. Alam and A. M. Abbosh, "Beam-steerable planar antenna using circular disc and four PIN-controlled tapered stubs for WiMAX and WLAN applications," *IEEE Antennas and Wireless Propagation Letters*, vol. 15, pp. 980–983, 2016.

[4] Y. Cai, S. Gao, Y. Yin, W. Li, and Q. Luo, "Compact-size low-profile wideband circularly polarized omnidirectional patch

antenna with reconfigurable polarizations," *IEEE transactions on Antennas and Propagation*, vol. 64, no. 5, pp. 2016–2021, 2016.

[5] M. Chen and C. Chen, "A compact dual-band GPS antenna design," *IEEE Antennas and Wireless Propagation Letters*, vol. 12, pp. 245–248, 2013.

[6] T. Guo, W. Leng, A. Wang, J. Li, and Q. Zhang, "A novel planar parasitic array antenna with frequency- and pattern-reconfigurable characteristics," *IEEE Antennas and Wireless Propagation Letters*, vol. 13, pp. 1569–1572, 2014.

[7] P. K. Li, Z. H. Shao, Q. Wang, and Y. J. Cheng, "Frequency and pattern reconfigurable antenna for multi-standard wireless applications," *IEEE Antennas and Wireless Propagation Letters*, vol. 14, pp. 333–336, 2015.

[8] Y. P. Selvam, M. Kanagasabai, M. G. N. Alsath et al., "A low-profile frequency- and pattern-reconfigurable antenna," *IEEE Antennas and Wireless Propagation Letters*, vol. 16, pp. 3047–3050, 2017.

[9] C. Sun, H. Zheng, L. Zhang, and Y. Liu, "Analysis and design of a novel coupled shorting strip for compact patch antenna with bandwidth enhancement," *IEEE Antennas and Wireless Propagation Letters*, vol. 13, pp. 1477–1481, 2014.

[10] R. Munson, "Conformal microstrip antennas and microstrip phased arrays," *IEEE Transactions on Antennas and Propagation*, vol. 22, no. 1, pp. 74–78, 1974.

[11] S. Chao, "Analysis and design of a compact circularly polarized microstrip antenna with cross-shape shorting strips," in *2015 IEEE International Conference on Communication Problem-Solving (ICCP)*, pp. 408–411, Guilin, China, 2015.

[12] C. Sun, H. Zheng, and Y. Liu, "Analysis and design of a low-cost dual-band compact circularly polarized antenna for GPS application," *IEEE Transactions on Antennas and Propagation*, vol. 64, no. 1, pp. 365–370, 2016.

[13] C. Sun, H. Zheng, L. Zhang, and Y. Liu, "A compact frequency-reconfigurable patch antenna for Beidou (COMPASS) navigation system," *IEEE Antennas and Wireless Propagation Letters*, vol. 13, pp. 967–970, 2014.

[14] H. A. Majid, M. K. A. Rahim, M. R. Hamid, and M. F. Ismail, "Frequency and pattern reconfigurable slot antenna," *IEEE Transactions on Antennas and Propagation*, vol. 62, no. 10, pp. 5339–5343, 2014.

[15] T. Li, H. Zhai, X. Wang, L. Li, and C. Liang, "Frequency-reconfigurable bow-tie antenna for bluetooth, WiMAX, and WLAN applications," *IEEE Antennas and Wireless Propagation Letters*, vol. 14, pp. 171–174, 2015.

[16] X. Wang, Y. Shang, and F. Shang, "A frequency reconfigurable antenna used for L band," in *2020 IEEE 3rd International Conference on Electronic Information and Communication Technology (ICEICT)*, pp. 208–210, Shenzhen, China, 2020.

[17] H. Pues and A. Van de Capelle, "Accurate transmission-line model for the rectangular microstrip antenna," *IEE Proceedings H*, vol. 131, no. 6, pp. 334–340, 1984.

[18] A. K. Bhattacharyya and R. Garg, "Generalized transmission line model for microstrip patches," *IEEE Proceedings*, vol. 132, pp. 93–98, 1985.

[19] R. L. Haupt and M. Lanagan, "Reconfigurable antennas," *IEEE Antennas and Propagation Magazine*, vol. 55, no. 1, pp. 49–61, 2013.